HEP'99 # 6_382
Submitted to Pa 6
Pl 6

DELPHI 99-68 CONF 255
15 June 1999

Measurement of the production of the four-fermion final states mediated by non-ZZ neutral current processes

Preliminary

DELPHI Collaboration

Paper submitted to the HEP'99 Conference
Tampere, Finland, July 15-21

Measurement of the production of the four-fermion final states mediated by non-ZZ neutral current processes

Preliminary

DELPHI Collaboration

R. Contri
INFN Genova
A. Lipniacka
Fysikum, University of Stockholm
T. Camporesi
CERN
K. Cieslik, H. Palka, M. Witek
Institute of Nuclear Physics, Krakow (supported in part by KBN Grant 2 P03B 111 16)
P. Bambade, G. Borisov, E. Ferrer Ribas, A. Stocchi
LAL, Orsay
M. E. Pol
CBPF, Rio De Janeiro
M. Begalli, L.M. Mundim
UERJ, Rio De Janeiro
H.T. Phillips
Rutherford Appleton Laboratory, Didcot
A. Baroncelli, E. Graziani, A. Passeri
Universita Roma III, Rome, Italy
A. Ballestrero
INFN Torino

Abstract

We report on the observation of the four-fermion final states originating from the neutral current processes, in the data sample collected by the DELPHI detector at the centre-of-mass energy of 188.6 GeV. The preliminary measurements of the differential cross-sections for the production of $\mu^+\mu^- q\bar{q}$, $e^+e^- q\bar{q}$ $l^+l^-l^+l^-$ and $\nu\bar{\nu}q\bar{q}$ final states outside the on-shell ZZ region have been compared with the Standard Model expectations.

1 Introduction

Four-fermion processes become increasingly important in e^+e^- interactions as the centre-of-mass energy increases. LEP provides a unique opportunity to test the Standard Model predictions for four-fermion interactions in several energy domains. Moreover, such processes form an irreducible background to new particle searches at LEP2 and a deviation from the Standard Model expectation would be a signal of new physics.

In this paper we report on the observation of the four-fermion final states originating from neutral current processes in the data sample collected at centre-of-mass energy of 188.6 GeV. ZZ production cross-section measurement have been reported elsewhere [1]. Preliminary measurements of the differential cross-sections for the production of $\mu^+\mu^-q\bar{q}$, $e^+e^-q\bar{q}$, $l^+l^-l^+l^-$ and $\nu\bar{\nu}q\bar{q}$ final states outside the on-shell ZZ region have been compared with the Standard Model expectations. For $\mu^+\mu^-q\bar{q}$ final states, a specially optimised analysis was carried out to measure the cross-section for the $Z\gamma^*$ process in that channel.

Outside the on-shell ZZ region, neutral-current four-fermion processes can be shown to be dominated by $Z\gamma^*$ production, whenever there are no electrons/positrons in the final states. Interference effects are small in this case. The cross-section for $Z\gamma^*$ production depends strongly on the mass of the γ^*, reaching approximately 120 pb for the real γ. A measurement of this cross-section has to be performed for the specific selection on the γ^* mass. For final states with electrons, other processes such as t-channel γ exchange accompanied by Z^*/γ^*-strahlung contribute significantly.

2 Detector description

A summary of the properties of the DELPHI detector relevant to this analysis is presented below. A more detailed description can be found in [2].

Charged particle tracks were measured in a system of cylindrical tracking chambers immersed in a 1.2 T solenoidal magnetic field. These were the Microvertex Detector (VD), the Inner Detector (ID), the Time Projection Chamber (TPC), and the Outer Detector (OD). In addition, two planes of drift chambers aligned perpendicular to the beam axis (Forward Chambers A and B) tracked particles in the forward and backward directions, covering polar angles $11° < \theta < 33°$ and $147° < \theta < 169°$.

The electromagnetic calorimetry consisted of the High density Projection Chamber (HPC) covering the barrel region of $40° < \theta < 140°$, the Forward ElectroMagnetic Calorimeter (FEMC) covering $11° < \theta < 36°$ and $144° < \theta < 169°$ and the STIC, a scintillator tile calorimeter which extends the coverage down to $1.66°$ in the forward and backward regions. The $40°$ taggers were a series of single-layer lead-scintillator counters used to veto electromagnetic particles otherwise missed in a region between HPC and FEMC. The hadron calorimeter (HCAL) covered 98% of the solid angle. Muons with momenta above 2 GeV can pass through the HCAL; these were recorded in a set of Muon Drift Chambers.

3 Data samples

In this paper the integrated luminosity of 158 pb^{-1} collected by the DELPHI detector at a centre-of-mass energy of 188.6 GeV was used. In the $\mu^+\mu^-q\bar{q}$ and $e^+e^-q\bar{q}$ channels the

54.0 pb^{-1} collected at 182.7 GeV centre-of-mass energy were used as well.

Simulated events were produced with the DELPHI simulation program DELSIM[3] and were then passed through the same reconstruction chain as the data. Processes leading to four-fermion final states were generated with EXCALIBUR[4], relying on JETSET 7.4 [5] for quark fragmentation. EXCALIBUR includes all tree-level diagrams in a consistent fashion. Initial state radiation was treated using the QEDPS program[6] for those final states which did not include e^+e^- pairs; for final states including e^+e^- the default EXCALIBUR collinear treatment was used.

Cuts were imposed at generator level on the invariant mass of fermion-antifermion pairs and on $\cos\theta_e$, the cosine of the angle of electrons relative to the electron beam and positrons relative to the positron beam. This was necessary because EXCALIBUR treats all fermions as having zero mass and hence the cross-sections diverge unless suitable cuts are applied. The requirements used at 188.6 GeV are shown in table 1.

GRC4F was used to generate four-fermion final states possible in the processes of $We\nu_e$ production with $\cos\theta_e > 0.9999$.

The background processes $e^+e^- \to f\bar{f}(n\gamma)$ were generated using PYTHIA [5]. Two-photon interactions were generated using TWOGAM [7] and BDK [8].

Quantity	Requirement
$\cos\theta_e$	< 0.98 in $e^+e^-l^+l^-$
$\cos\theta_e$	< 0.9999 otherwise
$E(e)$	> 1.0 GeV in $e^+e^-l^+l^-$ only
$M(e^+e^-)$	> 0.05 GeV/c^2
$M(\mu^+\mu^-)$	> 0.21 GeV/c^2
$M(\tau^+\tau^-)$	> 3.6 GeV/c^2
$M(d\bar{d})$	> 2 GeV/c^2
$M(u\bar{u})$	> 2 GeV/c^2
$M(s\bar{s})$	> 2 GeV/c^2
$M(c\bar{c})$	> 5 GeV/c^2
$M(b\bar{b})$	> 15 GeV/c^2

Table 1: Requirements made at generator level on electron/positron angles and masses of fermion-antifermion pairs for the EXCALIBUR samples used in the analysis at 188.6 GeV.

4 Jets and a pair of isolated leptons

The two final state leptons in the process $e^+e^- \to l^+l^-q\bar{q}$ are typically well isolated from all other particles. This property can be used to select such events with high efficiency in both the muon and electron channels[1]. Events were selected initially without explicit cuts on the masses of the final state fermion pairs in order to select ZZ, $Z\gamma^*$ events and other possible diagrams contributing like Ze^+e^- or t-channel γ^* exchange with Z/γ-strahlung. Mass cuts were then applied to isolate the $Z\gamma*$ component.

---

[1]Events with $\tau^+\tau^-$ pairs are not considered here.

The selection procedure for the $\mu^+\mu^- q\bar{q}$ and $e^+e^- q\bar{q}$ channels is almost the same and differs mainly in the numerical values of applied cuts.

Events were required to have at least 7 charged particles and a charged energy above $0.30 \sqrt{s}$. To suppress the radiative return to the Z the event was rejected if a photon with the energy more than 60 GeV was found or if the total missing momentum exceeded 50 GeV/c and absolute value of cosine of its polar angle exceeded 0.9.

Any charged particle with a momentum exceeding 5 GeV/c was considered as a possible lepton candidate. In the case of the electron channel to recover events in which the charged particle was not reconstructed, photons with energy between 20 GeV and 60 GeV were also considered as electron candidates.

Any neutral particle identified as a photon with energy greater than 0.5 GeV was combined with the lepton candidate if the invariant mass of the obtained cluster did not exceed $0.4\,\mathrm{GeV}/c^2$. At most two photons were included in such a cluster, the photon giving the smallest mass increase was added first. This procedure improved the measurement of the lepton energy in the events in which final state radiation or (in the case of electrons) bremsstrahlung occurred.

The direction of the lepton candidate was determined from the sum of momenta of the particles included in the so defined cluster and the energy was taken to be the sum of their energies. For electron candidates the value used for the energy of the charged particle was the greater of the energy deposited in the electromagnetic calorimeter and the momentum measured by the tracking system.

Events with at least two lepton candidates of the same flavour, opposite charge and invariant mass exceeding 2 GeV/c^2 were selected. All particles except the lepton candidates were clustered into jets using the JADE algorithm [11] with $y_{min} = 0.01$. A kinematic fit [10] including four-momentum conservation was applied to the event. Two discriminating variables for the selection of $l^+l^- q\bar{q}$ final state were defined, namely the transverse momentum, P_t, of a lepton candidate with respect to the nearest jet and the χ^2 per degree of freedom of the kinematic fit.

At least one of the two lepton candidates was required to satisfy strong lepton identification criteria. The other one was required to satisfy softer lepton identification criteria.

For muons strong identification criteria were that the momentum of the charged particle exceeded 5 GeV/c and that it was identified as a muon by the standard DELPHI identification package [2]. Softer identification criteria required that the momentum of the charged particle in the cluster exceeded 15 GeV/c, the energy deposited in the Electromagnetic Calorimeter did not exceed 30% of the charged particle momentum, energy deposited in the first layer of the Hadron Calorimeter did not exceed 25% of the charged particle momentum, and the total energy deposited in all calorimeters was less than 80% of the charged particle momentum.

The strong identification criteria for electrons were that the momentum of the charged particle in the cluster exceeded 5 GeV/c; energy deposited in the Electromagnetic Calorimeter exceeded 60% of the cluster energy or 15 GeV, the energy deposited in the first layer of the Hadron Calorimeter did not exceed 12 GeV and the energy deposited beyond the first layer of the Hadron Calorimeter did not exceed 15% of the cluster energy or 2.5 GeV.

To fulfil soft electron identification criteria the fraction of the energy of the cluster deposited beyond the first layer of the Hadron Calorimeter should not exceed 15%, and the momentum of the charged particle in the cluster had to be larger than 15 GeV/c.

The selections applied on the discriminating variables for the different final states are given in table 2.

lepton identification criteria	P_t^{min} (GeV/c)	$(\chi^2/\text{NDF})_{max}$
μ strong - μ strong	4.0	15.0
e strong - e strong	5.0	8.0
μ strong - μ soft	6.0	5.0
e strong - e soft	9.0	4.0

Table 2: Selection criteria for the different $l^+l^-q\bar{q}$ final states.

The $e^+e^-q\bar{q}$ final state contained more background coming from wrong electron identification and from photon conversions. To suppress this it was required that at least one of the electron candidates had either associated hits in the vertex detector or energy smaller than 60 GeV. In addition, if the transverse momentum of the electron candidate was less than 15 GeV/c, the total energy of the photons included in the electron cluster was required not to exceed 30% of the momentum of the electron candidate measured by the tracking system.

4.1 Results for the $l^+l^-q\bar{q}$ final state

The numbers of events observed before and after the mass selection are shown in table 3. The signal is defined as all $l^+l^-q\bar{q}$ events. The sample of events selected in the data collected at 182.7 GeV as described in [9] is presented here as well.

The predicted and observed distributions of the masses of the lepton and quark pairs for the $\mu^+\mu^-q\bar{q}$ and $e^+e^-q\bar{q}$ channels are shown in figure 1. The presence of the $Z\gamma^*$ contribution can be enhanced by requiring that one of the masses does not differ from M_Z by more than 20 GeV/c^2. If the mass of the hadronic system is required to be close to M_Z the mass distribution of the $\mu^+\mu^-$ pair has two distinct peaks, one close to zero and one close to M_Z, as shown in the upper left-hand side part of the figure 1. For the $e^+e^-q\bar{q}$ final states, there are less events predicted with M_{ee} close zero, and the mass distribution is flatter (lower left-hand side part of the figure 1) indicating the presence of non-resonant diagrams. The predicted and observed mass distribution of the quark pair for the mass of the lepton pair close to M_Z is shown in the right-hand side of the figure 1. There were less events in this selection, as expected from small leptonic branching ratio of the Z. Moreover, there were very few events with $M_{qq} < 30$ GeV/c^2 and M_{ll} close to M_Z demonstrating the dominance of the ZZ contribution for $Z \to l^+l^-$.

5 Dedicated selection of $\mu^+\mu^-q\bar{q}$ final states

As shown in the previous section, the particular case of the $\mu^+\mu^-q\bar{q}$ final state with a low mass $\mu^+\mu^-$ pair is dominated by the $Z\gamma^*$ process. Also more generally, the $\mu^+\mu^-q\bar{q}$ final state lends itself well to a decomposition in terms of $Z\gamma^*$ and ZZ components, because of the negligible interference and contribution from other processes.

Energy(GeV)	$\mu^+\mu^- q\bar{q}$			$e^+e^- q\bar{q}$		
	Data	Signal	Background	Data	Signal	Background
182.7	10	4.0 ± 0.3	0.38 ± 0.20	6	3.9 ± 0.3	0.55 ± 0.20
188.6	15	12.6 ± 0.1	0.81 ± 0.20	16	12.8 ± 0.1	1.43 ± 0.21

Table 3: The predicted numbers of signal and background events and the observed numbers of events in the $\mu^+\mu^- q\bar{q}$ and $e^+e^- q\bar{q}$ channels at 182.7 and 188.6 GeV centre-of-mass energies. The errors quoted are from simulation statistics.

In this section we describe an analysis dedicated to the $\mu^+\mu^- q\bar{q}$ final state, performed specially with the idea in mind of separating the $Z\gamma^*$ and ZZ components in the case of low $\mu^+\mu^-$ masses.

The analysis was based on the use of the sequential cuts listed below.

- The total charged multiplicity had to be larger than 7 and the total visible energy had to be larger than 80 GeV.

- The event had to have at least two well-identified muons with opposite charges and with an impact parameter measured with respect to the primary vertex smaller than 1 mm.

- No charged particle with a momentum of more than 2 GeV/c other than an identified muon was allowed to be in a cone of 0.4 rad constructed around each of the two identified muons.

- Each of the two identified muons had to have a momentum larger than 5 GeV/c.

- The sum of the momenta of the muons, $p_{\mu^+} + p_{\mu^-}$ had to be larger than 60 GeV/c.

- All charged parcticles other than identified muons were grouped in two jets and a constrained fit which imposes energy and momentum conservation was applied to the two muons of the selected pair and to the two jets.

The numbers of observed and expected events are shown in the table 4.

Energy(GeV)	$\mu^+\mu^- q\bar{q}$		
	Data	Signal	Background
182.7	8	4.5 ± 0.3	1.3 ± 0.20
188.6	14	9.9 ± 0.1	2.2 ± 0.20

Table 4: The predicted numbers of signal and background events and the observed numbers of events in the $\mu^+\mu^- q\bar{q}$ channel at 182.7 GeV and 188.6 GeV centre-of-mass energies. The errors quoted are from simulation statistics.

The efficiency for the $\mu^+\mu^- q\bar{q}$ final state depends on the invariant mass of the $\mu^+\mu^-$ system and ranges from 20 % for $M_{\mu^+\mu^-} \simeq 5$ GeV/c^2 to 40 % for $M_{\mu^+\mu^-} \simeq 20$ GeV/c^2 and 68 % for $M_{\mu^+\mu^-} > 60$ GeV/c^2.

5.1 Results of the dedicated analysis of $\mu^+\mu^- q\bar{q}$ final state

To separate ZZ and $Z\gamma^*$ contributions an unbinned likelihood fit was performed to the distribution of the events in the $M_{\mu^+\mu^-}$ vs M_{qq} plane.

The two dimensional distribution of those Monte Carlo signal events which passed the selection procedure described in section 5 was parametrised in the $M_{\mu^+\mu^-}$ vs M_{qq} plane. The ZZ component was parametrised as a two dimensional Gaussian distribution. The $Z\gamma^*$ component was parametrised as a superposition of three exponential distributions in the mass region well out of the ZZ peak. It was assumed that this component can be extrapolated under the ZZ peak. The small interference term and the background term were neglected.

These two parametrisations were then used as an input to the likelihood fit to the distribution of the data events in the $M_{\mu^+\mu^-}$ vs M_{qq} plane where the free parameters were numbers of events arising from ZZ and $Z\gamma^*$ contributions, N_{ZZ} and $N_{Z\gamma^*}$. We obtained

$$N_{Z\gamma^*} = 15.2 \pm 4.6$$

and

$$N_{ZZ} = 3.8 \pm 1.6.$$

After correcting for the average efficiency of 27 % for the $Z\gamma^*$ component and of 68 % for the ZZ component (and assuming that the ratio of cross-sections at 182.7 GeV and 188.6 GeV is described by EXCALIBUR), preliminary cross-sections for $\mu^+\mu^- q\bar{q}$ production at 188.6 GeV were obtained:

$$\sigma_{Z\gamma^* \to \mu^+\mu^- q\bar{q}} = 0.27 \pm 0.08 \; pb$$

and

$$\sigma_{ZZ \to \mu^+\mu^- q\bar{q}} = 0.031 \pm 0.013 \; pb.$$

This is in agreement with the EXCALIBUR prediction of $\sigma_{Z\gamma^* \to \mu^+\mu^- q\bar{q}} = 0.23 \; pb$ and $\sigma_{ZZ \to \mu^+\mu^- q\bar{q}} = 0.035 \; pb$ and with the result presented in [1].

The two projections of the fitted mass distribution along M_{qq} and $M_{\mu^+\mu^-}$ are shown in figure 2, upper and lower part respectively. In the figures the points indicate the data, darker shaded and lighter shaded histograms indicate the ZZ and $Z\gamma^*$ contributions respectively, the white histogram is the sum of them.

6 Four leptons

There are six possible four charged leptons final states: $e^+e^-e^+e^-$, $e^+e^-\mu^+\mu^-$, $e^+e^-\tau^+\tau^-$, $\mu^+\mu^-\mu^+\mu^-$, $\mu^+\mu^-\tau^+\tau^-$ and $\tau^+\tau^-\tau^+\tau^-$. Two types of analyses are reported in this paper. In the first analysis no attempt was made to identify lepton flavour in the final state ("flavour blind analysis"). The second analysis was directed to identify specifically $e^+e^-\mu^+\mu^-$ final states.

The event selection for both analyses has been restricted to topologies with four well reconstructed charged particles with momenta greater than 2 GeV/c (henceforth called lepton candidates). No more than four other charged particles, with momenta less than 2 GeV/c were allowed, implying that in the $e^+e^-\tau^+\tau^-$, $\mu^+\mu^-\tau^+\tau^-$ and $\tau^+\tau^-\tau^+\tau^-$ cases only one-prong decays of the τ were considered. The lepton candidates had to have total

charge equal to zero and an angle between momentum directions of any two of them had to be larger than 5°. The invariant mass of the pair of oppositely charged lepton candidates with the smallest opening angle was required to be greater than 1.5 GeV/c^2, in order to eliminate γ conversions.

"flavour blind analysis"

In the "flavour blind analysis" the four lepton candidates had to fulfil the following additional selection criteria, namely the total energy carried by them had to be greater than 50 GeV and no other two lepton candidates should be in a cone of 30° around any lepton candidate. These selections were applied to reject background from two-photon interactions and $\tau^+\tau^-(\gamma)$ final states.

The efficiency for this selection and the expected signal were extracted from the EXCALIBUR Monte Carlo for the six processes under study.

The Monte Carlo simulations used to estimate the background included two-fermion final states, two-photon interactions and all other four-fermion precesses, simulated as described in the section 3.

The expected EXCALIBUR cross-section, the efficiency for each channel normalised to the solid angle of 4π, the number of predicted signal events and the expected number of background events are shown in table 5. The most important contribution to the background was found to be the one coming from $\gamma\gamma \to q\bar{q}$.

	σ [pb]	ϵ (%)	expected events
$\mu^+\mu^-\mu^+\mu^-$	0.017	26.5	0.74
$e^+e^-e^+e^-$	0.420	3.7	2.46
$\tau^+\tau^-\tau^+\tau^-$	0.005	15.3	0.13
$e^+e^-\mu^+\mu^-$	0.389	5.6	3.43
$e^+e^-\tau^+\tau^-$	0.084	9.8	1.30
$\mu^+\mu^-\tau^+\tau^-$	0.022	11.0	0.38
Signal	0.937	7.3	8.44±1.30
Background			0.41±0.04
Total			8.85±1.30
DATA			10

Table 5: EXCALIBUR prediction for cross-section, the selection efficiency and expected number of events for signal and background for the "flavour blind" four leptons analysis

search for $e^+e^-\mu^+\mu^-$ final states

In the dedicated search for $e^+e^-\mu^+\mu^-$ final states two lepton candidates of opposite charge were required to be identified as $\mu^+\mu^-$ and the other two as e^+e^-. The following identification procedure was applied:

- Muon identification: the particles had to have associated hits in the Muon Chambers and the energy deposition and shower profiles in the Electromagnetic and Hadron Calorimeters were required to be compatible with a minimum ionising particle.

- Electron identification: there should not have been any signal in Muon Chambers nor any energy in the Hadron Calorimeter deposited after the first layer associated to the electron candidates. The energy in the Electromagnetic Calorimeter deposited in a 2° cone surrounding the particle had to be larger than 1 GeV.

The efficiency, expected number of events from the signal and expected background was determined using the same sample of simulated Monte Carlo as in the "flavour blind" analysis, with the final states $\mu^+\mu^-\mu^+\mu^-$, $e^+e^-e^+e^-$, $\tau^+\tau^-\tau^+\tau^-$, $e^+e^-\tau^+\tau^-$ and $\mu^+\mu^-\tau^+\tau^-$ now considered as background. The largest contribution to the background came from $e^+e^-\tau^+\tau^-$ and $\mu^+\mu^-\tau^+\tau^-$. The results of the selection are shown in table 6.

	σ [pb]	ϵ (%)	expected events
$e^+e^-\mu^+\mu^-$	0.389	6.5	4.00±0.12
Background			0.14±0.03
Total			4.14±0.12
DATA			4

Table 6: EXCALIBUR prediction for cross-section, the selection efficiency and expected number of events for signal and background for $e^+e^-\mu^+\mu^-$ final state.

6.1 Results for the four charged lepton channel

The cross-section was calculated taking into account the background and efficiency. Only statistical errors are quoted below.

In the "flavour blind" analysis ten events were selected in the data. The sum of the invariant masses of the two lepton pairs for the selected events in data, the Monte Carlo signal and background are shown in figure 3. The cross-section for the "flavour blind" four leptons processes was found to be

$$\sigma = (0.83 \pm 0.24)pb$$

in agreement with the EXCALIBUR prediction of 0.937 pb.

Four events were found in the data in the $e^+e^-\mu^+\mu^-$ analysis. The sum of the calculated effective masses for the selected events in data, the Monte Carlo signal and background are shown in figure 4.

The cross-section for production $e^+e^-\mu^+\mu^-$ final states was found to be

$$\sigma = (0.38 \pm 0.18)pb$$

again in agreement with the EXCALIBUR prediction of 0.39 pb.

7 The $q\bar{q}\nu\bar{\nu}$ channel

In the $q\bar{q}\nu\bar{\nu}$ channel the ZZ contribution dominates over the $Z\gamma^*$ one. For M_{qq} between 2 GeV/c^2 and the kinematical limit EXCALIBUR predicts a cross-section of 0.26 pb in

this channel with 0.18 pb coming from the ZZ (NC02) contribution. However, the ZZ contribution is expected to be negligible for 2 GeV/c^2 < M_{qq} < 60 GeV/c^2. Moreover $Z\gamma^*$ mediated $q\bar{q}\nu\bar{\nu}$ final states have characteristic signature of "monojets", with a low invariant mass hadronic system arising from the γ^* hadronization. When the γ^* mass is close to that of the Vector Mesons, processes like $\gamma^* \to \rho \to \pi\pi$ can be observed. The total cross-section for $q\bar{q}\nu\bar{\nu}$ in the region of for $2M_\pi < M_{qq} < 2$ GeV/c^2 can be obtained assuming hadron-parton duality and was estimated to be 0.0822±0.0017 pb (using `KORALW`) [12]. To model correctly final states arising in this case non-perturbative effects have to be included (eg. Vector Meson Dominance modelling). Simplified modelling of the γ^* fragmentation was used for the purpose of this paper. It was assumed that for $2M_\pi < M_{qq} < 2$ GeV/c^2 only $\gamma^* \to \rho \to \pi^+\pi^-$ takes place. The pion form factor measured as $R_\pi = \sigma(e^+e^- \to \pi^+\pi^-)/\sigma(e^+e^- \to \mu^+\mu^-)$ was used to model invariant mass distribution of $\pi^+\pi$ pairs.

Two analyses were performed. The first one is optimised for the low mass of the hadronic system, and it was used to search for events with $\gamma^* \to \rho \to \pi^+\pi^-$. The other one was used in the region of $M_{\gamma^*} > 2$ GeV/c^2. Both analyses are optimised to be efficient on $Z\gamma^*$. The efficiency goes to zero for $M_{qq} > 60$ GeV/c^2, where the ZZ contribution is expected.

In the first analysis at least two charged tracks with momentum greater than 400 MeV/c were required. Events containing identified electrons and muons were rejected, in order to suppress WW background and photon conversion background. The energy reconstructed in the STIC was required to be less than 10 GeV. The transverse momentum was required to be larger than 10 GeV/c. The total momentum in the event had to exceed 40 GeV/c. The polar angle of the missing momentum had to be in the range of $25° - 155°$. Finally, the event had to be strongly unbalanced. Two hemispheres were defined, according to the direction of the thrust axis: the energy in one of them had to account for at least 99% of the total energy in the event.

The efficiency of this selection for the $\nu\bar{\nu}\rho \to \pi^+\pi^-$ was 8.5 %.

A different analysis was used in for monojets with invariant mass greater than 2 GeV/c^2: Events with more than seven particles, more than five charged particles and total energy greater than 35 GeV were selected. The total momentum component parallel to the thrust axis had to exceed 35 GeV/c, and the total momentum component perpendicular to the beam axis (p_t) had to be greater than 10 GeV/c. In order to suppress $e^+e^- \to e^+e^-$ background, events with the total energy registered in electromagnetic calorimeters exceeding 90 % of the centre-of-mass energy were rejected. Events with electrons in the in the polar angle region $\theta < 15°$ and $\theta > 165°$, events with the most energetic electron or photon in the polar angle region $\theta < 10°$ and $\theta > 170°$ and events with an electron or a photon with energy greater than 45 GeV were rejected as well. If there was more than one electron or photon reconstructed in the event, the energy of the second most energetic one had to be smaller than 10 GeV. Moreover, events with energy deposited in the STIC in excess of 10 GeV were rejected. The selections listed above reject two-fermion and two-photon background.

All particles in the event were clustered into two jets using the DURHAM [13] algorithm and only the events with the angle between the two jets less than 50° and the separation parameter $y < 0.005$ were retained. The more energetic of the two jets were required to have an energy smaller than 70 GeV. A jet energy dependent selection on the number of charged particles in the most energetic jet was performed, jets with more

energy were required to contain more charged particles, so that average fraction of jet energy corresponding to one charged particle did not exceed 6 GeV.

The selection efficiency for the $q\bar{q}\nu\bar{\nu}$ channel was approximately 10% for $5\,\text{GeV}/c^2 < M_{qq} < 10\,\text{GeV}/c^2$, approximately 30% for $10\,\text{GeV}/c^2 < M_{qq} < 30\,\text{GeV}/c^2$ and zero for $M_{qq} > 40\,\text{GeV}/c^2$.

7.1 Results for the $q\bar{q}\nu\bar{\nu}$ channel

In the low mass analysis, two events were selected, with an expected background of 0.3 events. One of them is shown in figure 5. Two energetic charged particles are observed with invariant mass compatible with that of $\rho(770)$ and with energy deposit in the HCAL consistent with what is expected for pions.

In the other analysis, 6 events were selected in the data and 6.6 events in the Monte Carlo. Out of 6.6 Monte Carlo events, 2.6 were expected to result from $q\bar{q}\nu\bar{\nu}$ process, 1.1 events from the $e\nu q\bar{q}$ process, 2.1 events from the two-photon interactions and 0.6 events from two-fermion final states. One events selected in the data is shown in figure 6. It is a clear monojet event, with the jet reconstructed in the barrel region of the DELPHI detector.

8 Conclusions

We have searched for events produced by neutral-current processes different from ZZ in the $e^+e^-q\bar{q}$, $\mu^+\mu^-q\bar{q}$, $l^+l^-l^+l^-$ and $q\bar{q}\nu\bar{\nu}$ final states using data samples collected by the DELPHI detector at centre-of-mass energy of 188.6 GeV.

The results agree with the Standard Model predictions. The presence of $Z\gamma^*$ contribution to $e^+e^-q\bar{q}$, $\mu^+\mu^-qq$ and $q\bar{q}\nu\bar{\nu}$ final states was clearly demonstrated. We have measured the $Z\gamma^*$ to the $\mu^+\mu^-q\bar{q}$ final state to be

$$\sigma_{Z\gamma^* \to \mu^+\mu^-q\bar{q}} = .27 \pm 0.08 \; pb$$

for $M_{qq} > 2\,\text{GeV}/c^2$ and $M_{\mu\mu} > 2m_\mu$. This result is in agreement with the EXCALIBUR prediction of 0.23 pb.

References

[1] R. Jacobsson *et al.*, DELPHI Collaboration, *Measurement of the on-shell ZZ production cross-section at LEP 2*, contributed paper # 6_430 to the HEP'99 Conference, Tampere (1999).

[2] DELPHI Collaboration, P.Abreu *et al.*, Nucl. Instr. and Meth. **A378** (1996) 57.

[3] DELSIM *Reference Manual*, DELPHI note, DELPHI 87-97 PROG-100

[4] F.A. Berends, R. Pittau, R. Kleiss, Comp. Phys. Comm. **85** (1995) 437–452.

[5] T. Sjöstrand, Comp. Phys. Comm. **39** (1986) 347; T. Sjöstrand, PYTHIA 5.6 *and* JETSET 7.3, CERN-TH/6488-92.

[6] Y.Kurihara, J. Fujimoto, T. Munehisa, Y. Shimizu, KEK CP-035, KEK 95-126 (1995).

[7] S.Nova, A.Olshevski, and T. Todorov, *A Monte Carlo event generator for two photon physics*, DELPHI note 90-35 PROG 152.

[8] F. A. Berends, P. H. Daverveldt, R. Kleiss, Comp. Phys. Comm. **40** (1986) 271-284, 285-307, 309-326

[9] D. Fassouliotis *et al.*, DELPHI Note 97-100 CONF 91, submitted to Jerusalem conference.
P. Bambade *et al.*, DELPHI 98-104 CONF 172, submitted to ICHEP'98, Vancouver.

[10] see section 5.2 in P. Abreu *et al.* E. Phys. J. **C2** (1998) 581.

[11] T. Sjöstrand, Comp. Phys. Comm. **28** (1983), 229.

[12] S. Jadach,W. Placzek, M. Skrzypek, B.F. Ward and Z. Was. Comput. Phys. Commun. **119** (1999) 1.

[13] S. Catani, Yu.L. Dokshitzer, M. Olson, G. Turnock and B.R. Webber, Phys. Lett. **B269** (1991) 432.
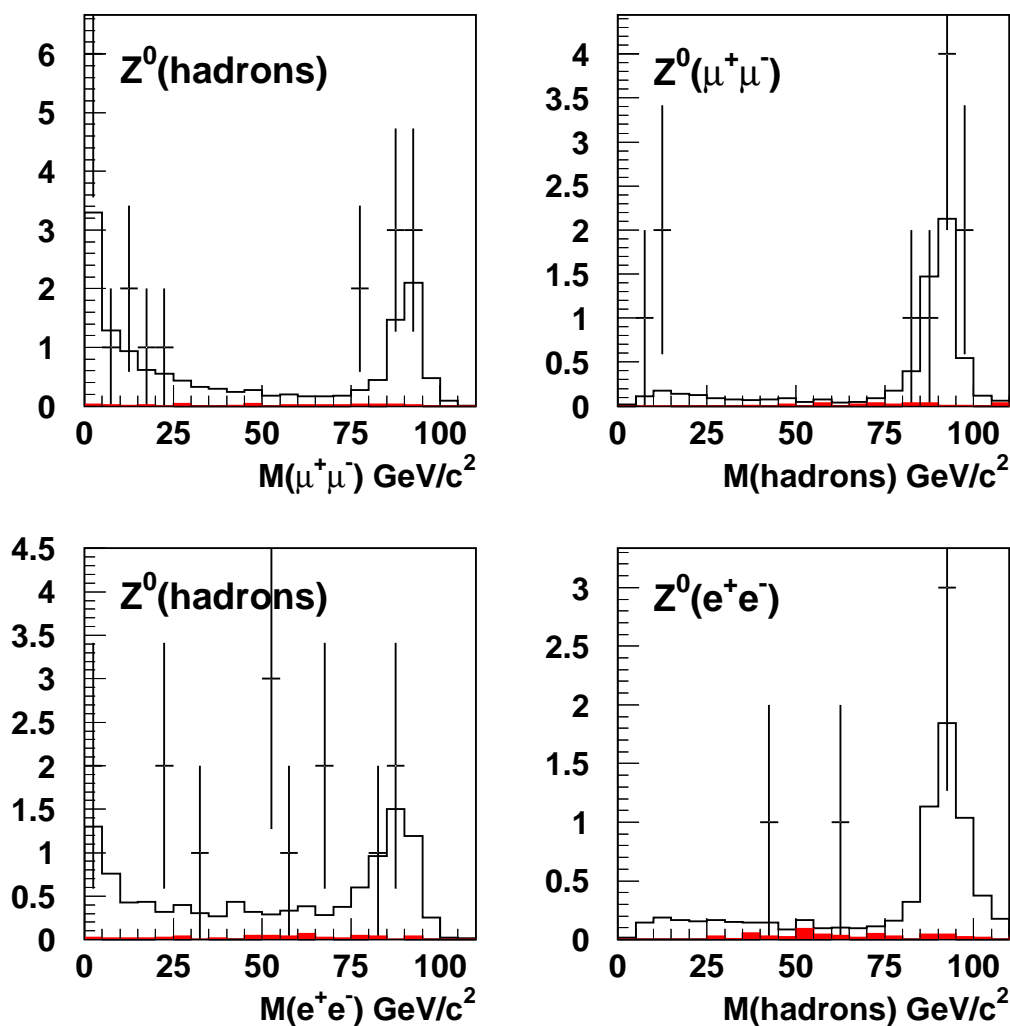
Figure 1: Distributions of the mass of one fermion pair when the mass of the second is close M_Z. The two lower plots are for the $e^+e^- q\bar{q}$ channel and two upper plots for $\mu^+\mu^- q\bar{q}$ channel. The points are the data, the empty histogram is the prediction of the simulation and the filled histogram is the contribution of the background.
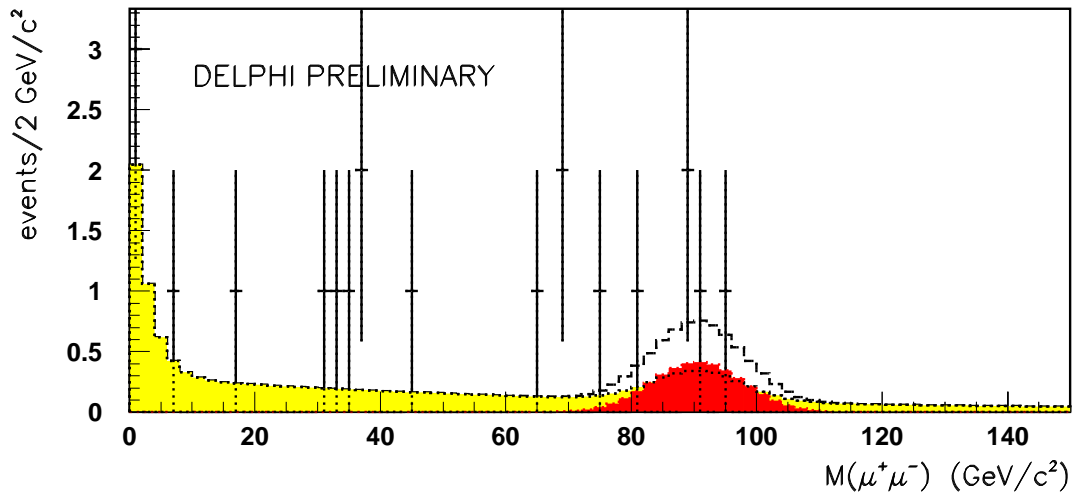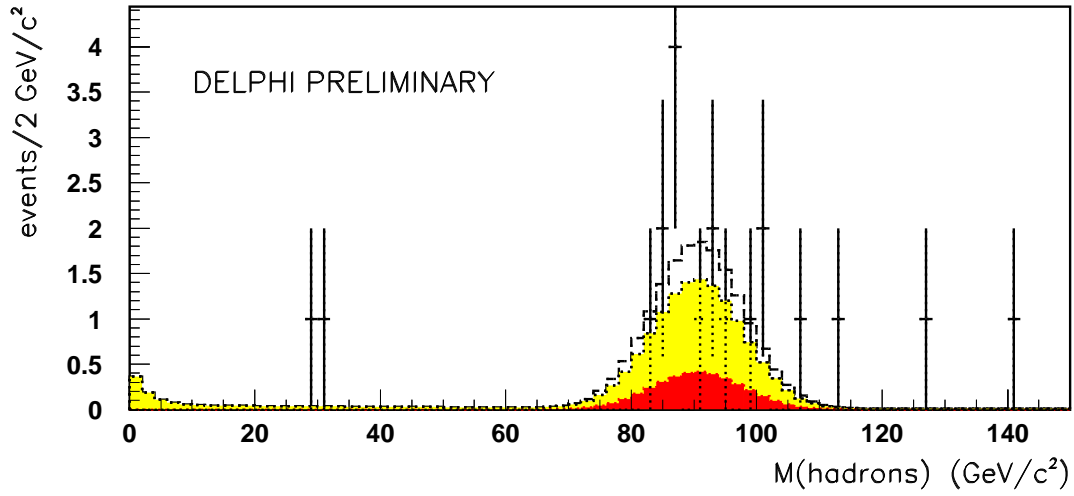
Figure 2: upper plot:M_{qq} distribution for the $\mu^+\mu^- q\bar{q}$ channel. Lower plot:$M_{\mu^+\mu^-}$ distribution. Points indicate the data, dark shaded and light shaded histograms indicate the ZZ and $Z\gamma^*$ contributions respectively, white histogram is the sum of ZZ and $Z\gamma^*$.
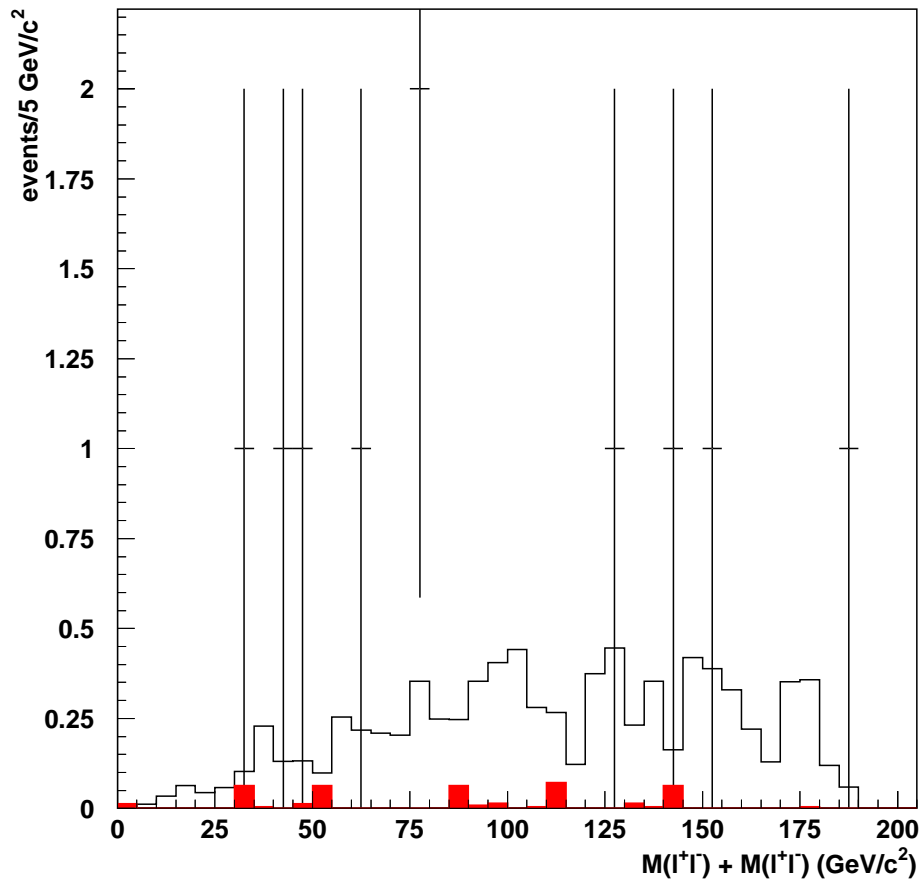
Figure 3: Sum of the invariant masses of the two lepton pairs, for the events selected in the "flavour blind" four-lepton analysis at 188.6 GeV. Out of the two possible pairing configurations of oppositely charged leptons the one which was giving the largest $M_{l^+l^-} + M_{l^+l^-}$ was chosen. The points are the data, the histogram is the prediction from simulation. The shaded region indicates the predicted contribution from background processes.
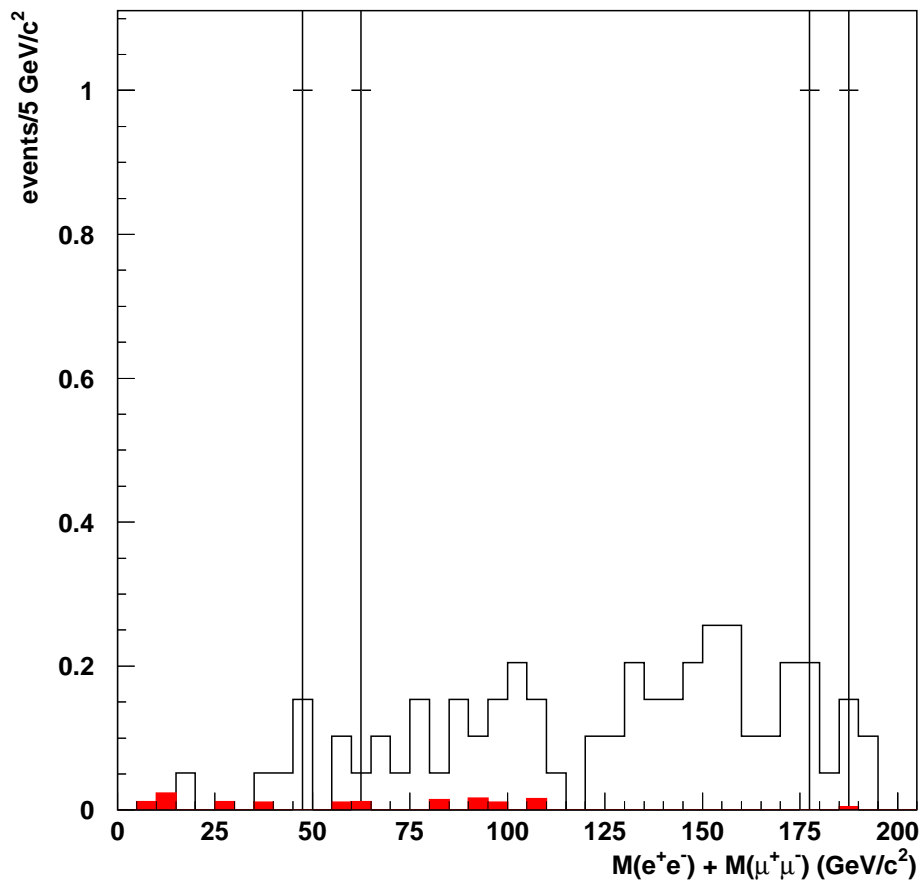
Figure 4: Sum of the invariant masses of the two lepton pairs, for the events selected in the $e^+e^-\mu^+\mu^-$ analysis at 188.6 GeV. The points are the data, the histogram is the prediction from simulation. The shaded region indicates the predicted contribution from background processes.
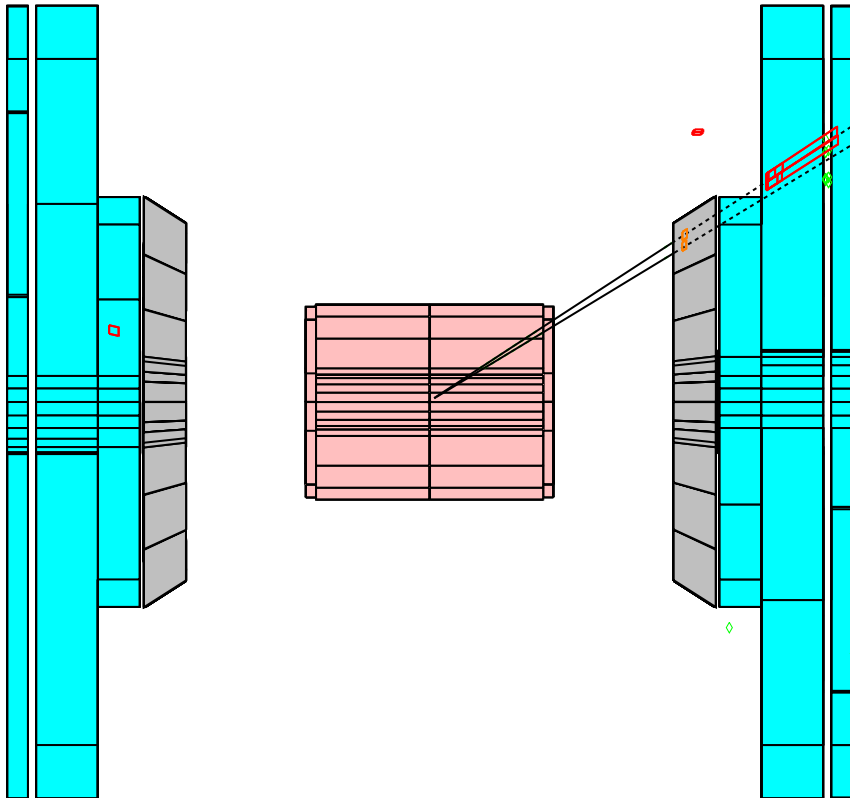
Figure 5: One of the $\nu\bar{\nu}\pi^+\pi^-$ candidate events selected at 188.6 GeV centre-of-mass energy. The energy deposited by two charged particles in the hadronic calorimeter is consistent with expectations for pions.
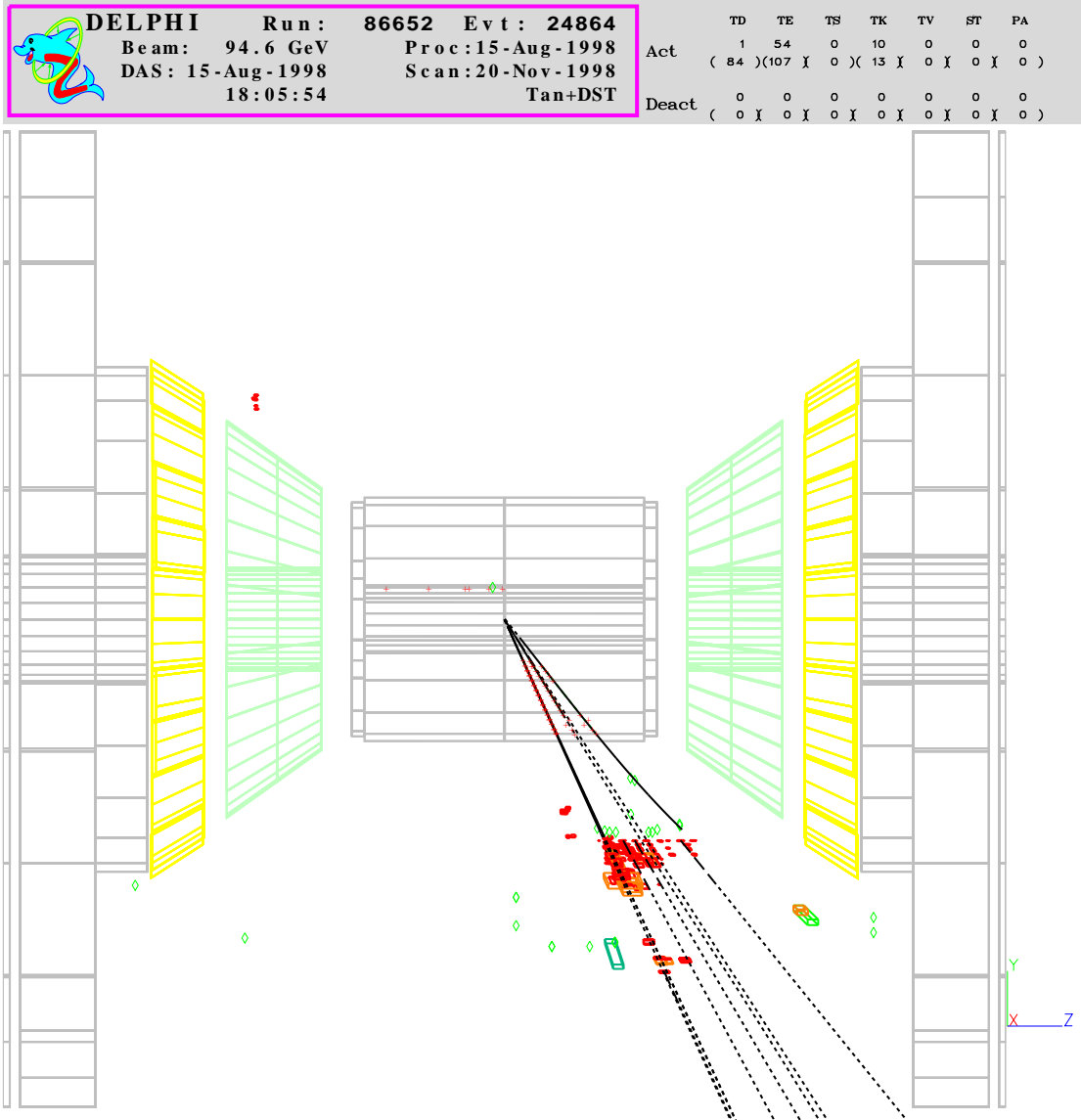
Figure 6: One of the $\nu\bar{\nu}q\bar{q}$ "monojet" candidate events selected at 188.6 GeV centre-of-mass energy.